Medical Radiology
Series Editors: H.-U. Kauczor · H. Hricak · M. Knauth

U. Joseph Schoepf
Felix G. Meinel *Editors*

Multidetector-Row CT of the Thorax

Second Edition

Springer

Medical Radiology

Diagnostic Imaging

For further volumes:
http://www.springer.com/series/4354

U. Joseph Schoepf • Felix G. Meinel
Editors

Multidetector-Row CT of the Thorax

Second Edition

Springer

Editors
U. Joseph Schoepf
Department of Radiology and
Radiological Science
Medical University of South Carolina
Charleston, SC
USA

Felix G. Meinel
Institute for Clinical Radiology
Ludwig-Maximilians-University Hospital
Munich
Germany

ISSN 0942-5373 ISSN 2197-4187 (electronic)
Medical Radiology
ISBN 978-3-319-30353-6 ISBN 978-3-319-30355-0 (eBook)
DOI 10.1007/978-3-319-30355-0

Library of Congress Control Number: 2016944609

Printed on acid-free paper

This Springer imprint is published by Springer Nature
The registered company is Springer International Publishing AG Switzerland

To Our Patients

Foreword

The first edition of "MDCT of the Thorax" was published in 2004 when the new capabilities and clinical applications of MDCT were met with excitement and explored with great enthusiasm. Since then, much has happened – the excitement has persisted and has even grown. While 16-row scanners were once celebrated as the peak of innovation in 2004, 64-row computed tomography is now considered to be standard technology with 128 and even 320-row scanners available in the high-end sector. However, the technical innovations are by no means limited to the number of detector rows. Iterative reconstruction methods, new detector materials, automated tube current modulation and tube voltage selection have substantially reduced the radiation exposure to patients. These improvements mitigate and perhaps invalidate the primary argument against the widespread use of CT angiography of the coronary arteries in particular.

For the second edition, editors Joseph Schoepf and Felix Meinel have kept important features essential to the success of the first edition while revising and updating each chapter to capture the rapidly advancing developments in CT and their clinical applications. New chapters have been added, including: "Dual Energy CT of the Thorax", "Comprehensive CT Imaging in Acute Chest Pain", and "Imaging of the Heart-Lung Axis". In contrast, chapters from the first edition which have since lost their importance have been excluded.

The editors are to be congratulated on assembling an authorial team of highly recognized, international experts. Furthermore, one has to thank the authors for illustrating that the technical and methodological advancements of the recent past are not just improvement for improvement's sake, but significantly increase the clinical applicability and the diagnostic value of MDCT.

It can be asserted with good reason that MDCT of the thorax is one of the most interesting and exciting fields of radiology. Few topics in medical imaging arouse such heated discussion as lung cancer screening with CT or the use of CT in acute chest pain. This work provides detailed, comprehensive information on these and many other topics that capture the cutting-edge of innovation while remaining valuable for everyday practice.

I would like to sincerely thank the editors, authors, and Springer for promoting this important work and I wish them much deserved success. I have no doubt that readers will not only enjoy the book, but also find it a significant help in their daily practice.

Munich, Germany
March 2016

Maximilian F. Reiser

Preface

...δὶς ἐς τὸν αὐτὸν ποταμὸν οὐκ ἂν ἐμβαίης...

It has been more than a decade since the first edition of this tome – and what an amazing 12 years it has been for a spectacular medical imaging modality and those who harness its power! Not only is CT not dead, as it was quite ubiquitously predicted and accepted at the eve of the last millennium, but rather it has piled triumph upon roaring triumph in our conquest of disease. And hardly any other area of CT imaging has seen more dramatic evolution, more spectacular victories, or more profound disruption than the evaluation of the cardiothoracic system. The scourges of the past were utterly and effectively vanquished: Pulmonary embolism has found its match, eradicating the diagnostic uncertainties from days past. Heart disease is increasingly tackled by the new, imposing kid on the block – cardiac CT. Doubts over the effectiveness of CT lung cancer screening have all but disappeared and this test is shaping up as a powerful weapon in our war on cancer. And the list goes on…

Our exploits can in part be ascribed to the ingenuity, curiosity, and zeal of the radiological community in the pursuit of ever more refined strategies to better the fate of our patients. But our intellect and our passion alone would have stood little chance to overcome our formidable adversaries. To our aid came the brilliance of engineers, thinkers, technical innovators, who gave us the means, gave us the tools, the very instruments of success. Zooming through the chest in a split second, freezing the heart's motion, obtaining tissue signatures of organs healthy and diseased, smoking out pathology with micrometer precision – what a feat!

As with the first edition, we were able to assemble a stellar team of global experts, fabled bards to sing the stories of our exploits, to chronicle our journey, and to take tally of the spoils of war on human ailment. Again, the result of our collective musing has become a shining testimony to the prowess of our profession and a reflection of our ever increasing abilities in medicine. Our deep gratitude goes out to our many friends who dedicated their precious time and their genius to the success of this work. We thank the editorial team at Springer, who again so expertly steered the publication of this new edition. Lastly, we salute our patients, who are the reason for it all.

Charleston, South Carolina, USA — U. Joseph Schoepf
Munich, Germany — Felix G. Meinel
March 2016

Contents

Part III Lung Nodules/Lung Cancer

Part IV Cardiovascular Applications

Part V Data Management

Part VI Miscellaneous

Contributors

Vartika Appiah Department of Radiology, Epicura – Hopital de la Madeleine, Ath, Belgium

Edwin J.R. van Beek Clinical Research Imaging Centre, University of Edinburgh, Edinburgh, Scotland, UK

Clinical Research Imaging Centre, The Queen's Medical Research Institute, Edinburgh, UK

Catherine Beigelman-Aubry Diagnostic and Interventional Radiology, University Hospital Lausanne, Lausanne, Switzerland

Chandra Bortolotto Department of Thoracic Imaging, Hospital Calmette (EA 2694), University of Lille Nord de France, Lille, France

Yolonda L. Colson Division of Thoracic Surgery, Brigham and Women's Hospital and Harvard Medical School, Boston, MA, USA

Anand Devaraj Department of Radiology, Royal Brompton Hospital, London, UK

Julien Dinkel Institute for Clinical Radiology, Ludwig-Maximilians-University Hospital, Munich, Germany

Shannon G. Farmakis St. Louis University School of Medicine, SSM Health Cardinal Glennon Children's Hospital, Saint Louis, MO, USA

John Field Department of Molecular and Clinical Cancer Medicine, The University of Liverpool, Institute of Translational Medicine, Liverpool, UK

Dominik Fleischmann Department of Radiology, Stanford University School of Medicine, Stanford, CA, USA

Thomas G. Flohr Siemens Healthcare GmbH, Computed Tomography, CT Concepts Department, Forchheim, Germany

Department of Interventional Radiology, Eberhard-Karls-University, Tübingen, Germany

Matthew K. Fuld Diagnostic Imaging, Computed Tomography, Collaborations, Siemens Medical Solutions, Inc, Malvern, PA, USA

Stephen R. Fuller Department of Radiology and Radiological Science, Medical University of South Carolina, Charleston, SC, USA

Camilo A. Garcia Service de Médecine Nucléaire, Université Libre de Bruxelles, Institut Jules Bordet, Brussels, Belgium

Victor H. Gerbaudo Division of Nuclear Medicine and Molecular Imaging, Brigham and Women's Hospital, Harvard Medical School, Boston, MA, USA

Pierre Alain Gevenois Department of Radiology, Hôpital Erasme, Université libre de Bruxelles, Brussels, Belgium

Lucas L. Geyer Institute for Clinical Radiology, LMU Ludwig-Maximilians-University Hospital Munich, Munich, Germany

Ritu R. Gill Department of Radiology, Brigham and Women's Hospital and Harvard Medical School, Boston, MA, USA

Jin Mo Goo Department of Radiology, Seoul National University Hospital, Jongno-gu, Seoul, South Korea

Jochen M. Grimm Department of Medical Radiology, University Hospital Center and University of Lausanne, Lausanne, Switzerland

University Center of Legal Medicine Lausanne/Geneva, Lausanne, Switzerland

Maxime Hackx Department of Radiology, Hôpital Erasme, Université libre de Bruxelles, Brussels, Belgium

Richard L. Hallett Cardiovascular Imaging, Northwest Radiology Network, Indianapolis, IN, USA

Division of Cardiovascular Imaging, Department of Radiology, Stanford University School of Medicine, Stanford, CA, USA

Ethan J. Halpern Department of Radiology, Thomas Jefferson University, Philadelphia, PA, USA

Marieke Hovinga Department of Radiology, Meander Medical Center, Amersfoort, The Netherlands

Bertram Jobst Department for Diagnostic and Interventional Radiology, University Hospital Heidelberg, Heidelberg, Germany

Willi A. Kalender Institute of Medical Physics, University of Erlangen-Nürnberg, Erlangen, Germany

Rashmi Katre Department of Radiology, The University of Texas Health Science Center at San Antonio, San Antonio, TX, USA

Hans-Ulrich Kauczor Department of Diagnostic and Interventional Radiology, University Hospital Heidelberg, Heidelberg, Germany

Tatiana Kelil Department of Radiology, Brigham and Women's Hospital and Harvard Medical School, Boston, MA, USA

Suonita Khung Department of Thoracic Imaging, Hospital Calmette (EA 2694); Univ Lille Nord de France, Lille, France

Chang Hyun Lee Department of Radiology, College of medicine, Seoul National University, Seoul, South Korea

Michael M. Lell Department of Radiology, Friedrich-Alexander University Erlangen-Nürnberg, Erlangen, Germany

Ulrich Linsenmaier Institute for Diagnostic and Interventional Radiology, HELIOS Kliniken München WEST and HELIOS Kliniken München Perlach and Klinikum Augustinum München, Munich, Germany

Stefanie Mangold Department of Radiology and Radiological Science, Medical University of South Carolina, Charleston, SC, USA

Department of Diagnostic and Interventional Radiology, University Hospital of Tuebingen, Tuebingen, Germany

Felix G. Meinel Institute for Clinical Radiology, Ludwig-Maximilians-University Hospital, Munich, Germany

Hagen Meredig Department of Diagnostic and Interventional Radiology, University Hospital Heidelberg, Heidelberg, Germany

Saeed Mirsadraee Clinical Research Imaging Centre, University of Edinburgh, Edinburgh, Scotland, UK

Clinical Research Imaging Centre, The Queen's Medical Research Institute, Edinburgh, UK

Amy Mumbower Department of Radiology, The University of Texas Health Science Center at San Antonio, San Antonio, TX, USA

Matthijs Oudkerk Department of Radiology, University of Groningen, University Medical Center Groningen, Center for Medical Imaging – North East Netherlands, Groningen, The Netherlands

Julien Pagniez Department of Thoracic Imaging, Hospital Calmette (EA 2694); Univ Lille Nord de France, Lille, France

Narinder S. Paul Department of Medical Imagining, Toronto General Hospital, University Ave, University of Toronto, Toronto, ON, Canada

Robin Peters Department of Radiology, University of Groningen, University Medical Center Groningen, Center for Medical Imaging – North East Netherlands, Groningen, The Netherlands

Jim Potchen Department of Radiology, Michigan State University, East Lansing, MI, USA

Juan Carlos Ramirez-Giraldo Diagnostic Imaging, Computed Tomography, Collaborations, Siemens Medical Solutions, Inc., Malvern, PA, USA

James G. Ravenel Department of Radiology and Radiological Science, Medical University of South Carolina, Charleston, SC, USA

Jacques Remy Department of Thoracic Imaging, Hospital Calmette (EA 2694); Univ Lille Nord de France, Lille, France

Martine Remy-Jardin Department of Thoracic Imaging, Hospital Calmette (EA 2694); Univ Lille Nord de France, Lille, France

Carlos S. Restrepo Department of Radiology, The University of Texas Health Science Center at San Antonio, San Antonio, TX, USA

Carole A. Ridge Department of Radiology, Mater Misericordiae University Hospital, Dublin, Ireland

Beth A. Ripley Department of Radiology, Brigham and Women's Hospital and Harvard Medical School, Boston, MA, USA

Geoffrey D. Rubin Department of Radiology, Duke University School of Medicine, Durham, NC, USA

Cornelia Schaefer-Prokop Department of Radiology, Meander Medical Center, Amersfoort, The Netherlands

Department of Radiology, Radboud University Nijmegen, Nijmegen, The Netherlands

Sabine Schmidt Diagnostic and Interventional Radiology, University Hospital Lausanne, Lausanne, Switzerland

Bernhard Schmidt Siemens Healthcare GmbH, Computed Tomography, CT Concepts Department, Forchheim, Germany

U. Joseph Schoepf Department of Radiology and Radiological Science, Medical University of South Carolina, Charleston, SC, USA

Marilyn J. Siegel Mallinckrodt Institute of Radiology, Washington University School of Medicine, St Louis, MO, USA

Stephen B. Solomon Department of Radiology, Memorial Sloan Kettering Cancer Center, New York, USA

Ralf Sprengers Department of Radiology, Meander Medical Center, Amersfoort, The Netherlands

Denis Tack Department of Radiology, Epicura – Hopital de la Madeleine, Ath, Belgium

Rozemarijn Vliegenthart Department of Radiology, University of Groningen, University Medical Center Groningen, Center for Medical Imaging – North East Netherlands, Groningen, The Netherlands

Julian L. Wichmann Department of Radiology and Radiological Science, Medical University of South Carolina, Charleston, SC, USA

Department of Diagnostic and Interventional Radiology, University Hospital Frankfurt, Frankfurt, Germany

Mark O. Wielpütz Department for Diagnostic and Interventional Radiology, University Hospital Heidelberg, Heidelberg, Germany

Amelia M. Wnorowski Department of Radiology, Thomas Jefferson University, Philadelphia, PA, USA

Long Jiang Zhang Department of Medical Imaging, Jinling Hospital, Medical School of Nanjing University, Nanjing, China

MDCT – Technical Background, Radiation Protection

CT Technology for Imaging the Thorax: State of the Art

Thomas G. Flohr and Bernhard Schmidt

Abstract

We review the basics of CT system design, scan, and image reconstruction techniques, as well as scan protocols for imaging of the thorax with multidetector row CT (MDCT) systems. In addition, we discuss CT systems with wide area detectors and dual-source CT (DSCT). We briefly describe different techniques to reduce the radiation dose in thoracic CT, and we discuss dual energy CT acquisition techniques which have the potential to provide combined functional and morphological information, e.g., to depict local perfusion deficits in the lung parenchyma in patients with pulmonary embolism.

1 Introduction

The advent of spiral computed tomography (CT) in 1990 and the broad introduction of multidetector row computed tomography (MDCT) in 1998 were significant steps in the ongoing refinement of CT-imaging techniques of the thorax.

With the first generation of 4-slice CT systems, high-resolution imaging of the entire thorax within one breath-hold of the patient became feasible, and CT was quickly recognized as the gold standard for the diagnosis of pulmonary embolism up to the level of sub-segmental arteries (Schoepf et al. 2002; Remy-Jardin et al. 2002).

T.G. Flohr (✉)
Siemens Healthcare GmbH, Computed Tomography, CT Concepts Department, Forchheim, Germany

Department of Interventional Radiology, Eberhard-Karls-University, Tübingen, Germany
e-mail: thomas.flohr@siemens.com

B. Schmidt
Siemens Healthcare GmbH, Computed Tomography, CT Concepts Department, Forchheim, Germany

ECG-synchronized data acquisition (Ohnesorge et al. 2000), which proved to be sufficient for adequate visualization of the coronary arteries at low to moderate heart rates (Achenbach et al. 2000; Becker et al. 2000; Knez et al. 2001; Nieman et al. 2001), could unfortunately not be extended to the entire thorax because of slow scan speed.

The generation of 16-slice MDCT systems (Flohr et al. 2002a, b) provided simultaneous acquisition of 16 submillimeter slices and faster gantry rotation with rotation times down to 0.375 s. CT scans of the entire thorax with submillimeter spatial resolution were now possible in about 10 s. As a consequence, central and peripheral pulmonary embolism could be reliably and accurately diagnosed even in dyspneic patients with limited ability to cooperate (Remy-Jardin et al. 2002; Schoepf et al. 2003). The combined assessment of pulmonary embolism and deep venous thrombosis, first demonstrated in 2001 (Schoepf et al. 2001), entered clinical routine. The faster scan speed of ECG-gated cardiac scanning with 16 slices enabled motion-free visualiza-

U.J. Schoepf, F.G. Meinel (eds.), *Multidetector-Row CT of the Thorax*, Medical Radiology,
DOI 10.1007/978-3-319-30355-0_1

tion of the lung and the cardiothoracic vessels as well as cardiac functional evaluation in one scan, even though detailed visualization of the coronary arteries was still limited (Coche et al. 2005).

Sixty-four-slice CT systems, available since 2004, enabled CT imaging of the thorax with isotropic submillimeter spatial resolution in less than 5 s scan time. This facilitated the examination of uncooperative patients and emergency patients, e.g., with suspicion of acute pulmonary embolism. The improved temporal resolution due to gantry rotation times down to 0.33 s increased the clinical robustness of ECG-gated scanning at higher heart rates, even though most authors still proposed the administration of beta-blockers (Leber et al. 2005; Raff et al. 2005). Sixty-four-slice CT scanners enabled comprehensive diagnosis of morphology and cardiac function within one integrated CT examination, including high-resolution imaging of the coronary arteries (Salem et al. 2006; Bruzzi et al. 2006a, b; Delhaye et al. 2007). ECG-gated 64-slice CT was also used for rapid triage of patients with acute chest pain in the emergency room and for diagnosis of pulmonary embolism, aortic dissection or aneurysm, or significant coronary artery disease in one scan. This application is often referred to as "triple rule out" (Schoepf 2007; Johnson et al. 2007a). As a downside, ECG-gated MDCT scanning of the entire thorax can result in considerable radiation exposure, which is of particular concern in patients with low likelihood of disease.

Even with 64-slice CT, motion artifacts remained an important challenge for cardiothoracic imaging. In 2005, a dual-source CT (DSCT) system, i.e., a CT system with two x-ray tubes and two corresponding detectors offset by 90°, was introduced (Flohr et al. 2006). It provided improved temporal resolution of 83 ms independent of the patient's heart rate as compared to 165–190 ms with MDCT systems at that time. DSCT scanners proved to be well suited for integrated cardiothoracic examinations even in acutely ill patients and for the triage of patients with acute chest pain (Johnson et al. 2007b). The introduction of dual-energy scanning with DSCT enabled tissue characterization and provided combined functional and morphological information, e.g., to depict local perfusion deficits in the lung parenchyma in patients with pulmonary embolism (Pontana et al. 2008; Thieme et al. 2008).

The second and third generations (introduced in 2009 and 2013, respectively) of DSCT systems offer high-pitch scan modes which enable high-resolution CT scans of the entire thorax in less than 1 s scan time with an acquisition time per image better than 100 ms (Lell et al. 2009; Tacelli et al. 2010). These scan modes are potentially advantageous for evaluating the lung parenchyma and vascular structures in patients who have difficulty complying with breath-holding instructions (Schulz et al. 2012). High-pitch scan modes have been used for fast CTA scans of the aorta (Beeres et al. 2012). Combined with ECG triggering, they provide adequate visualization of the coronary arteries, the aorta, and the iliac arteries in one scan at low radiation dose, which is beneficial in the planning of transcatheter aortic valve replacement (TAVR) procedures (Wuest et al. 2012; Plank et al. 2012).

Since 2009, iterative reconstruction techniques have been used to significantly reduce the radiation dose in CT examinations of the thorax (e.g., Prakash et al. 2010; Leipsic et al. 2010; Pontana et al. 2011a, b, 2015; Singh et al. 2011; Baumueller et al. 2012). With the latest generation of iterative reconstruction and dedicated pre-filtration of the x-ray beam, radiation dose values of 0.1 mSv and less have been reported for non-enhanced CT scans of the thorax (Newell et al. 2015).

Yet another challenge for CT is the visualization of dynamic processes in extended anatomical ranges, e.g., to characterize the inflow and outflow of contrast agent in the arterial and venous systems in dynamic CT angiographies or to determine the enhancement characteristics of the contrast agent in volume perfusion studies. One way to address this problem is the introduction of area detectors large enough to cover organs such as the heart, the kidneys, or the brain in one axial scan. Meanwhile, two vendors have introduced CT scanners with 16 cm detector coverage at isocenter, providing 320×0.5 mm collimation at 0.27 s rotation time or 256×0.625 mm collimation at 0.28 s rotation time. These scanners have the potential to acquire dynamic volume data by repeatedly scanning the same anatomical range without table movement (e.g., Ohno et al. 2011; Willems et al. 2012; Motosugi et al. 2012). An alternative to provide time-resolved CT data of larger anatomical volumes is a periodic shuttle movement of the patient table while scan data are acquired (e.g., Goetti

et al. 2012; Morhard et al. 2010; Sommer et al. 2010, 2012). This technique is realized in several CT systems with smaller detector *z*-coverage.

Overall, the greatest challenge of evolving CT technology is the explosion of information now available to physicians. Standardizing the display of post-processed images will be increasingly important to preserve efficient workflow and optimum patient care.

2 CT System Technology

2.1 Multi-Detector Row CT (MDCT)

In this section, we review the basics of CT system design, scan, and image reconstruction techniques, as well as scan protocols for imaging of the thorax with multi-detector row CT (MDCT) systems. In our terminology, these are CT systems with 2–128 detector rows and a detector *z*-coverage of up to 8 cm at isocenter. CT systems with wider detectors (e.g., 320×0.5 mm or 256×0.625 mm, both covering 16 cm) and dual-source CT (DSCT) systems will be discussed in a separate section because of their different clinical protocols.

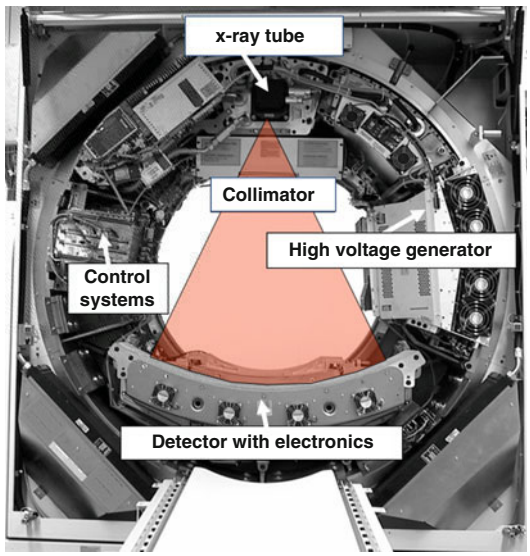

Fig. 1 Basic system components of a modern MDCT system. The x-ray fan beam is indicated in red; it covers a SFOV of typically 50 cm in diameter. The data measurement system consists of detector and detector electronics

2.1.1 MDCT System Design

The basic system components of a modern MDCT system are shown in Fig. 1. Today, the third-generation fan-beam CT design is used by all manufacturers, characterized by an x-ray tube and an opposing detector which are mounted on a rotating gantry ring. The detector is a two-dimensional array, consisting of 2–128 rows aligned in the *z*-axis direction (the *z*-axis is the patient's longitudinal axis) with 700 and more detector elements in each row. The fan angle of the detector is wide enough (approximately 45–55°) to cover a whole-body scan field of view (SFOV) of usually 50 cm in diameter. In a CT scan, the detector array measures the x-ray attenuation profile of the patient at about 1000–2000 different angular positions during a 360° rotation. All measurement values acquired at the same angular position of the measurement system are called a "projection" or "view." Slip-ring designs which pass the electrical signals across sliding contacts allow for continuous rotation of the measurement system.

State-of-the art x-ray tubes are powered by onboard generators and provide peak powers of 60–120 kW at different user-selectable voltages ranging from 80 to 140 kV. Recently, the available voltage range was extended to enable new clinical applications, and other tube voltages such as 70 kV became available. Scanning at low tube voltage is favorable for dose-efficient pediatric CT (Niemann et al. 2014; Durand and Paul 2014). In addition, contrast-enhanced examinations can be performed at reduced radiation dose and potentially reduced amount of contrast agent, because the x-ray attenuation of iodine significantly increases at lower kV (Meyer et al. 2014). This technique will be described in detail in Sect. 3.1.

All modern MDCT systems use solid-state scintillation detectors. The x-rays hit a radiation-sensitive crystal or ceramic (such as gadolinium oxide, gadolinium oxysulfide, or garnets) with suitable doping. They are absorbed, and their energy is converted into visible light which is detected by a Si photodiode attached to the backside of the detector. The resulting electrical current is amplified and converted into a digital signal.

Key requirements for a detector material are good detection efficiency, i e., high atomic number, and very short afterglow time to enable fast

readout at the high gantry rotation speeds that are essential for cardiothoracic CT.

The image noise in a CT image is caused by the quantum noise of the x-ray photons and the electronic noise of the detection system. In high-dose scanning situations, the image noise is dominated by quantum noise. Electronic noise significantly contributes to the image noise when bigger patients are scanned or in examinations at low radiation dose, e.g., in low-dose thorax scans. In addition, electronic noise degrades image quality and the stability of CT values. Recently, a detector with integrated electronics was commercially introduced (STELLAR, Siemens Healthcare, Forchheim, Germany), with the goal to reduce electronic noise and detector cross talk. In this design, photodiodes and analog-to-digital converters are combined and directly attached to the ceramic scintillators, without the need of noise-sensitive analog connection cables (see Fig. 2). In a recent study, image noise reduction by up to 40 % for a 30 cm phantom corresponding to an average abdomen was demonstrated with the use of a detector with integrated electronics at 80 kV (Duan et al. 2013). According to the authors, this noise reduction translated into up to 50 % in dose reduction to achieve equivalent image noise.

A CT scanner must provide different slice widths to adapt scan speed and through-plane (z-axis) resolution to the clinical requirements of different scan protocols. In MDCT, detectors with a larger number of detector rows than finally read-out slices are used to provide slices

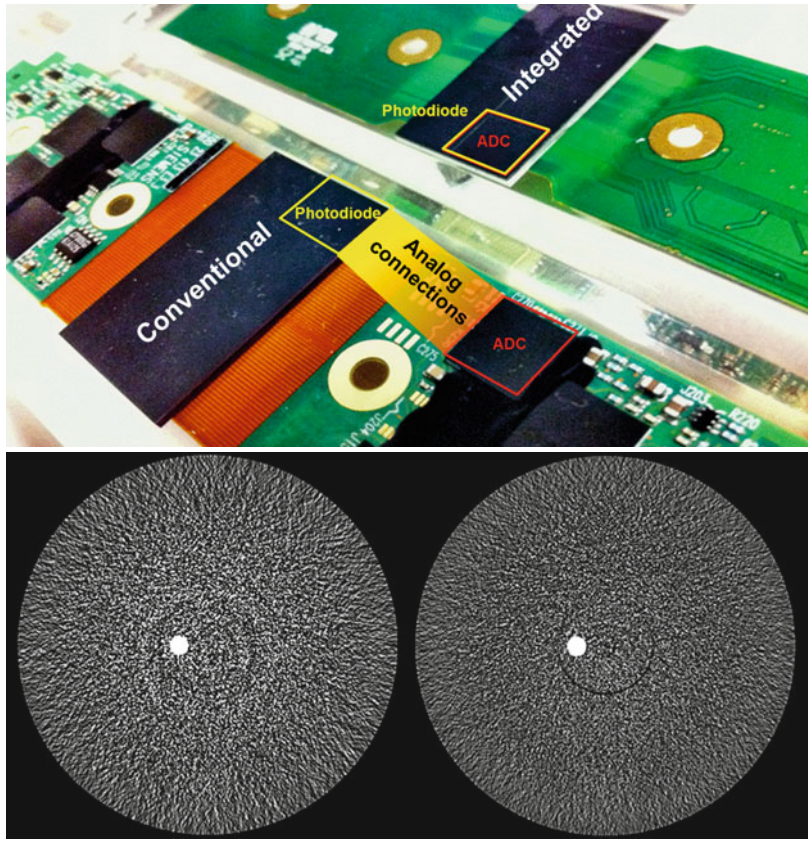

Fig. 2 *Top*: Principle of an integrated CT detector compared to a conventional CT detector. The Si tile is shown without the scintillation ceramics. Integrated detectors do not use distributed electronics with analog connections. As a consequence, electronic noise and cross talk are reduced. *Bottom*: Image quality improvement in a 40 cm phantom with an integrated detector (*right*) as compared to a conventional detector (*left*). Scan parameters: 80 kV, 100 mAs

at different collimated slice widths. The total beam width in the *z*-direction is adjusted by pre-patient collimation, and the signals of every two (or more) detectors along the *z*-axis are electronically combined to thicker slices.

The detector of a 16-slice CT (Siemens SOMATOM Emotion 16) as an example comprises 16 central rows, each with 0.6 mm collimated slice width, and four outer rows on either side, each with 1.2 mm collimated slice width – in total, 24 rows with a *z*-width of 19.2 mm at isocenter (Fig. 3). By adjusting the x-ray beam width such that only the central detector rows are illuminated, the system provides 16 collimated 0.6 mm slices (Fig. 3, top). By illuminating the entire detector, reading out all rows, and electronically combining the signals of every two central rows, the system provides 16 collimated 1.2 mm slices (Fig. 3, bottom). The 16-slice detectors of other manufacturers are similarly designed, with slightly different collimated slice widths (0.5, 0.6, or 0.625 mm, depending on the manufacturer).

MDCT detectors with 64 detector rows provide 64 collimated 0.5, 0.6, or 0.625 mm slices. They allow acquisition of 32 collimated 1.0, 1.2,

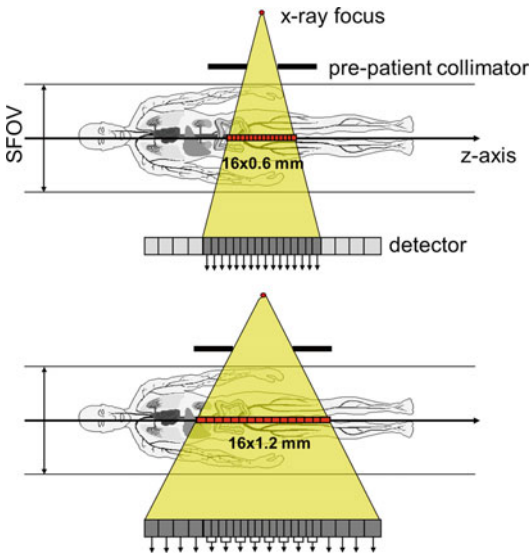

Fig. 3 Example of a 16-slice detector, which consists of 24 detector rows and provides either 16 collimated 0.6 mm slices (*top*) or – by combination of the signals of every two central rows – 16 collimated 1.2 mm slices (*bottom*)

or 1.25 mm slices by electronic combination of every two detector rows. One CT system has a detector with 128 collimated 0.625 mm slices (total *z*-width 8 cm at isocenter). The widest commercially available CT detectors cover 16 cm at isocenter; they acquire 320 collimated 0.5 mm slices (Aquilion ONE, Toshiba Medical, Japan) or 256 collimated 0.625 mm slices (Revolution, GE Healthcare, USA).

All modern MDCT scanners enable reconstruction of images with different slice widths from the same raw data – typically, the scan data are acquired at submillimeter collimation (e.g., 64×0.6 mm, or 64×0.625 mm), and different sets of image data are reconstructed with different target slice widths according to the clinical needs (e.g., 3 or 5 mm for initial viewing and additional submillimeter slices or 1 mm slices for post-processing).

Some CT systems double the number of simultaneously acquired slices by using special "conjugate" interpolation schemes during image reconstruction or by means of a *z*-flying focal spot (Flohr et al. 2004, 2005). The focal spot in the x-ray tube is periodically moved between two *z*-positions on the anode plate by electromagnetic deflection. As a consequence, the measurement rays of two readings are shifted by half a collimated slice width at isocenter and can be interleaved to one projection with double the number of slices, but half the *z*-sampling distance (Fig. 4). Two 64-slice readings with 0.6 mm slice width and 0.6 mm *z*-sampling distance, as an example, are combined to one projection with 128 overlapping 0.6 mm slices at 0.3 mm *z*-sampling distance.

The *z*-flying focal spot provides improved data sampling in the *z*-direction for better through-plane resolution and reduced spiral windmill artifacts (see Fig. 5).

2.1.2 MDCT Scan and Image Reconstruction Techniques

With the advent of MDCT, axial "step-and-shoot" scanning has remained in use for only few clinical applications, such as ECG-triggered cardiac scans at low radiation dose. For the vast majority of all MDCT examinations, spiral (helical) scanning is the method of choice.

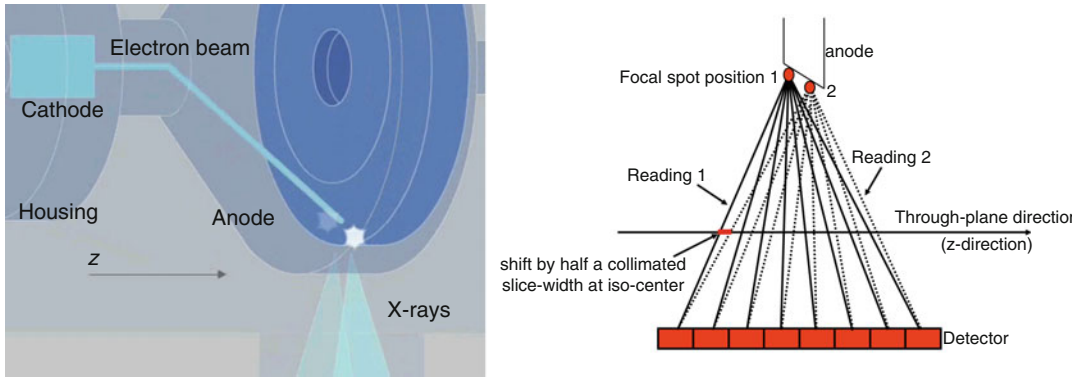

Fig. 4 Principle of a *z*-flying focal spot. Consecutive readings are shifted by half a collimated slice width (at isocenter) by means of a periodic motion of the focal spot on the anode plate. Every two readings are interleaved to one projection with double the number of slices and half the *z*-sampling distance

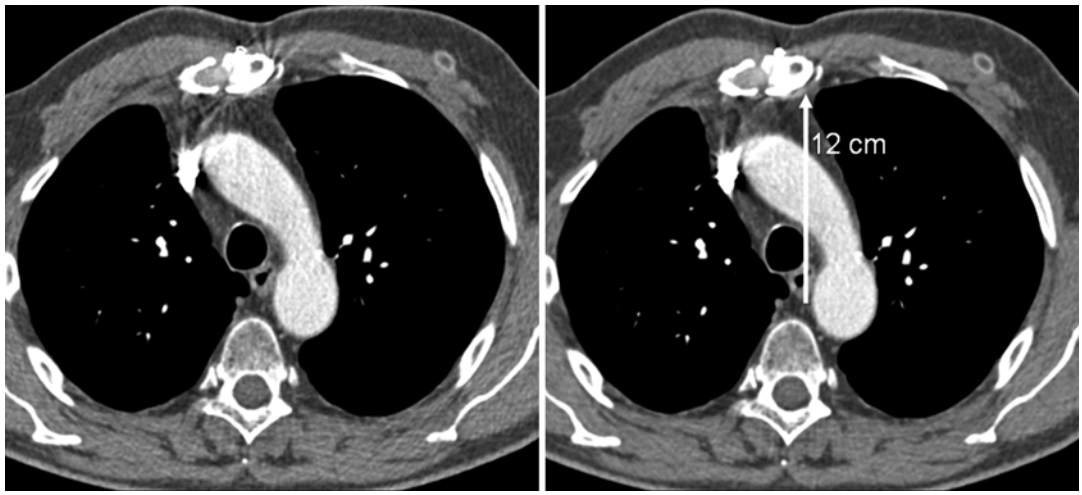

Fig. 5 Reduction of spiral windmill artifacts in a 64-slice CT scan (*left*) with the *z*-flying focal spot technique (*right, white arrow*). The distance of the sternum from the isocenter is about 12 cm

An important parameter to characterize a spiral scan is the pitch p. It is given by p = tablefeed per rotation/total z-width of the collimated beam at isocenter

This definition applies to single-slice CT as well as to MDCT. It indicates whether scan data are acquired with gaps ($p > 1$) or with overlap ($p < 1$) in the through-plane direction. If the x-ray tube current is left unchanged, radiation dose increases with decreasing pitch due to the overlapping radiation. Some CT scanners (e.g., Siemens MDCT systems) compensate for this increase by automatically lowering the tube current with decreasing pitch such that a constant; pitch-independent "reference mAs" and radiation dose are applied.

Many technical challenges of MDCT image reconstruction, such as the complicated z-sampling patterns or the cone-angle problem, have been addressed in the past 15 years. In two-dimensional image reconstruction approaches used for single-slice CT, all measurement rays are perpendicular to the z-axis. In MDCT systems, however, the measurement rays are tilted by the so-called cone angle with respect to a plane perpendicular to the z-axis. The wider the

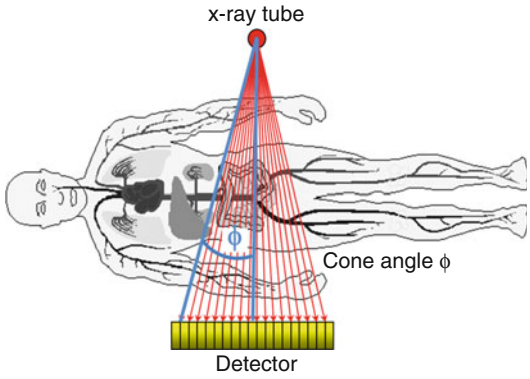

Fig. 6 Geometry of a MDCT scanner demonstrating the cone-angle problem: in the patient's longitudinal direction (z-direction), the measurement rays are tilted by the so-called cone-angle ϕ with respect to a plane perpendicular to the z-axis

detector is in the z-direction, i.e., the more detector rows it has, the larger is the cone angle of the outer detector rows (Fig. 6).

For CT systems with up to eight simultaneously acquired slices, cone-beam artifacts stay at a clinically acceptable level if the cone angle of the measurement rays is simply neglected in the image reconstruction algorithms. The rays are then treated as if they were perpendicular to the z-axis. For CT systems with more than eight slices, the cone angle has to be taken into account at least approximately. Pertinent reconstruction methods considering the cone-beam geometry are nutating slice algorithms (e.g., Flohr et al. 2003) and 3D-filtered back projection (Stierstorfer et al. 2004). Nowadays, 3D-filtered back projection is the reconstruction method of choice for most MDCT systems (Grass et al. 2000; Hein et al. 2003; Stierstorfer et al. 2004). 3D-filtered back projection is a natural extension of the 2D-filtered back projection used in single-slice CT reconstruction: the measurement rays are back projected into a 3D volume along the lines of measurement, in this way accounting for their cone-beam geometry. 3D-filtered back projection, even though it is an approximate algorithm, can significantly reduce cone-beam artifacts. In most MDCT scanners, 3D-filtered back projection is enhanced by z-filtering techniques which enable the reconstruction of images with different slice widths from the same CT raw data. The user can then trade off z-axis resolution with image noise.

2.1.3 Scan Protocols for MDCT Imaging of the Thorax

CT imaging of the thorax benefits from MDCT technology in several ways:

- *Shorter scan time*. Examination times for standard protocols can be significantly reduced. With modern MDCT systems, the entire thorax can be scanned at submillimeter isotropic resolution in less than 5 s. CT angiographic examinations benefit from these short scan times, because a compact contrast bolus may be used.
- *Extended scan range*. Larger scan ranges can be examined within one breath-hold time of the patient. This is relevant for CT angiography with extended coverage and for oncological staging. The chest and abdomen, as an example, can be examined in one scan with one contrast bolus.
- *Improved through-plane resolution*. The most important clinical benefit is the ability to scan a region of interest, e.g., the chest, within a breath-hold time of the patient with substantially thinner slices than in single-slice CT. The significantly improved through-plane resolution is beneficial for all reconstructions, in particular when 3D post-processing is part of the clinical protocol.

In clinical practice, most scan protocols benefit from a combination of these advantages. The close-to or true isotropic spatial resolution in routine examinations – depending on the number of detector rows – enables 3D renderings of diagnostic quality and oblique multiplanar reformations (MPRs) with a resolution comparable to the axial images. The wide availability of MDCT systems has transformed CT from a modality acquiring cross-sectional slices of the patient to a volume imaging modality. In many scan protocols, the use of narrow collimation is recommended independently of what slice width is desired for primary viewing. In practice, different

slice widths are commonly reconstructed by default: thick slices for PACS archiving and primary viewing and thin slices for 3D post-processing and evaluation.

MDCT imaging of the thorax also greatly benefits from the shorter gantry rotation times of modern MDCT scanners and the reduced acquisition times per image. The better the temporal resolution of the images, the less pronounced are motion artifacts in CT images of the thorax, which typically appear as double contours or blurring of thoracic structures close to the heart. The best possible temporal resolution in a single-source CT scan is half the rotation time of the respective scanner, because half a rotation of scan data is the minimum needed for image reconstruction close to the isocenter. CT scanners used for thoracic imaging should therefore enable short gantry rotation times – at the moment, rotation times of 0.25–0.3 s result in a best possible temporal resolution of 125–150 ms. A further significant improvement of the temporal resolution to values below 100 ms can be achieved with dual-source CT systems (see Fig. 7) (Adapted from Hutt et al. 2016).

It is interesting to note that the temporal resolution in a spiral scan, which is the basic scan mode for MDCT scanning of the thorax, depends on the pitch of the scan: the higher the pitch, the better the temporal resolution. At a pitch of 1, a full rotation of scan data typically contributes to an image. Temporal resolution is therefore not better than the gantry rotation time. The higher the pitch, the less data contribute to image reconstruction, and the temporal resolution approaches half the gantry rotation time. On the other hand, even lower pitch will lead to even worse temporal resolution: at a pitch of 0.5, almost two rotations of scan data contribute to an image. Therefore, to reduce motion artifacts, it is mandatory to perform MDCT examinations of the thorax at fast gantry rotation and high pitch >1. Another option, in particular when the heart and the coronary arteries are also targeted in the planned examination, is the use of ECG-gated scan protocols. As a downside, these protocols result in longer scan times and increased radiation dose to the patient. ECG-triggered high-pitch scan protocols are a potential way out of this dilemma – they will be discussed in Sect. 2.3.

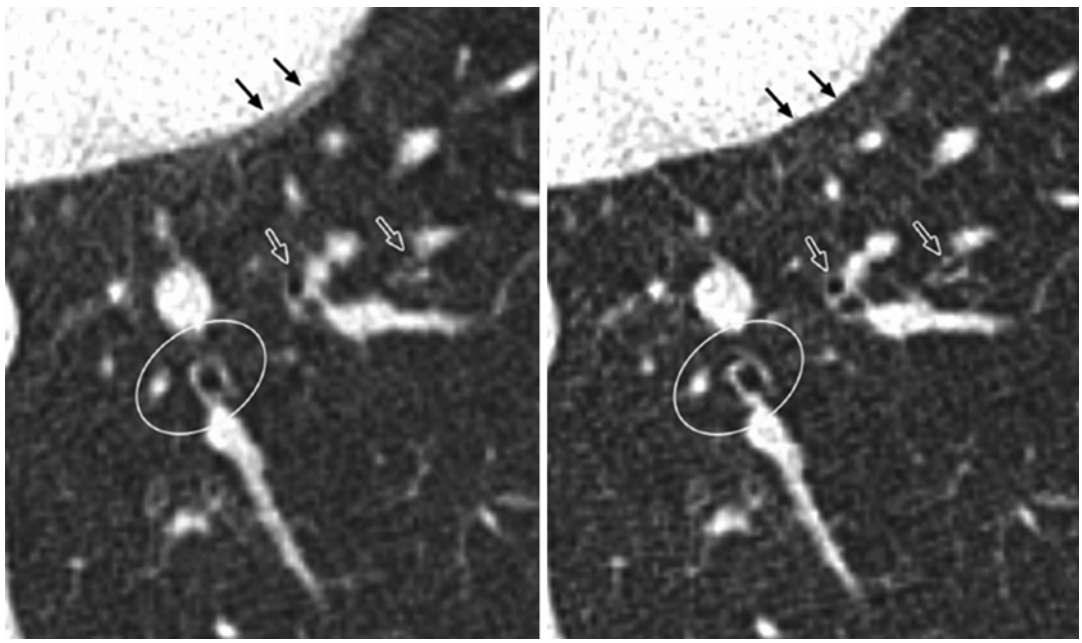

Fig. 7 Lung image acquired with a dual-source CT and reconstructed at a temporal resolution of 140 ms (*left*) and 75 ms (*right*). Note the double contour of the left ventricular wall due to cardiac motion (*fine arrows*) and the blurry appearance of the bronchi (*arrows*) in the image at 140 ms temporal resolution (Modified from (Hutt et al. 2016))

2.2 CT Systems with Area Detector

An area detector is a CT detector wide enough in the through-plane (z-axis) direction to cover entire organs, such as the heart, the kidneys, or the brain, in one axial scan without table movement. Two commercially available CT systems provide 16 cm detector coverage at isocenter, either with a collimation of 320×0.5 mm and 0.27 s rotation time (Aquilion ONE, Toshiba Medical Systems, Japan) or with 256×0.625 mm and 0.28 s rotation time (Revolution, GE Healthcare, USA). The SFOV is cone shaped in the z-axis direction (see Fig. 8).

CT scanners with area detectors are optimized for axial scanning without table movement – this scan technique has benefits in ECG-controlled cardiac imaging and in the acquisition of dynamic CT data, e.g., of the brain. Larger scan volumes in the z-direction, e.g., the entire thorax, have to be covered by "stitching," i.e., by appending axial scans shifted in the z-direction. With increasing SFOV, more overlap in the z-direction is required for gapless volume coverage. Another option is standard spiral scanning. Then, however, only a smaller detector coverage of, e.g., 80 mm is typically available because of image reconstruction challenges, and the maximum table feed is limited to, e.g., 300 mm/s.

In ECG-controlled cardiac CT imaging, an image stack with an anatomical coverage corresponding to the detector z-width is acquired in each heartbeat. Typical MDCT detectors provide a z-coverage of 40 mm (and recently up to 80 mm) at isocenter, so two to four of these image stacks acquired in two to four consecutive heartbeats have to be put together to a volume image of the heart (Flohr et al. 2007). These image stacks can be blurred or shifted relative to each other as a consequence of insufficient temporal resolution or variations of the heart motion from one cardiac cycle to the next, resulting in stair-step or banding artifacts. CT systems with 16 cm detector coverage avoid these artifacts, because they can scan the entire heart in one axial scan without table movement (Rybicki et al. 2008). As a downside, all images will be affected in case of arrhythmia or ectopic beats during data acquisition. Another challenge of larger detectors is increased x-ray scatter. Scattered radiation may cause hypodense cupping or streaking artifacts, and the scatter-induced noise may reduce the contrast-to noise-ratio (CNR) in the images (Flohr et al. 2009a). Meanwhile, successful use of CT systems with 16 cm detector coverage for coronary CTA and other cardiac applications has been demonstrated (Rybicki et al. 2008; Steigner et al. 2009; Dewey et al. 2009). The application spectrum has been extended to, e.g., scanning of patients with atrial fibrillation (Kondo et al. 2013)

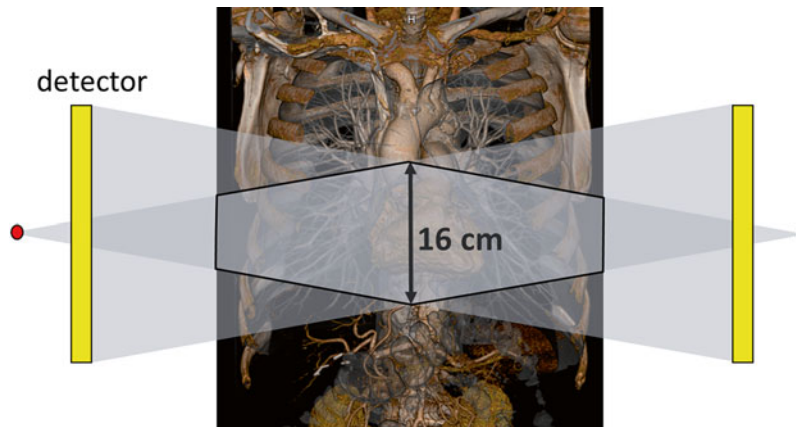

Fig. 8 Schematic illustration of axial CT scanning with a CT system with an area detector wide enough to cover entire organs such as the heart. Two commercially available CT systems provide 16 cm z-coverage at isocenter

and coronary CTA combined with the first-pass perfusion evaluation (George et al. 2015; Sharma et al. 2015). The second generation of 320-row CT scanners has been shown to enable coronary CTA at reduced radiation dose compared to the first generation (Tomizawa et al. 2013; Chen et al. 2013).

As a second benefit, CT systems with area detectors can acquire dynamic volume data by repeatedly scanning the same anatomical range without table movement. This is useful in dynamic CT angiographic examinations, e.g., in patients with brain arteriovenous malformations (Willems et al. 2012) or in volume perfusion studies, e.g., of the brain (Manniesing et al. 2016). In the context of thoracic scanning, 320-detector row first-pass perfusion scanning has been used to differentiate between malignant and benign pulmonary nodules (Ohno et al. 2011).

In triple-rule-out acute chest pain evaluation, the use of the sequential wide-volume mode proved to be more dose efficient than standard spiral scanning (Kang et al. 2012).

2.3 Dual-Source CT

A dual-source CT (DSCT) is a CT system with two x-ray tubes and two detectors at an angle of about 90° (see Fig. 9). Both measurement systems acquire CT scan data simultaneously at the same anatomical level of the patient (same *z*-position).

The first generation of DSCT scanners with 2×64 slices and 0.33 s gantry rotation time was introduced in 2006 (Somatom Definition, Siemens Healthcare, Forchheim, Germany), the second generation with 2×128 slices and 0.28 s gantry rotation time in 2009 (Somatom Definition Flash, Siemens Healthcare, Forchheim, Germany), and the third generation with 2×192 slices and 0.25 s gantry rotation time in 2014 (Somatom Definition Force, Siemens Healthcare, Forchheim, Germany).

DSCT systems provide significantly improved temporal resolution for cardiothoracic imaging. The shortest data acquisition time for an image corresponds to a quarter of the gantry rotation time. Close to the isocenter, 180° of scan data is the minimum needed for image reconstruction. Due to the 90° angle between both x-ray tubes, each of the measurement systems needs to acquire only 90° of scan data. The two 90° segments at the same anatomical level are put together to the 180° scan. Using this technique, a temporal resolution of 83, 75, and 66 ms, respectively, is achieved for the three generations of DSCT systems. With the dual-source approach, temporal resolution is independent of the patient's heart rate, because data from one cardiac cycle only are used to reconstruct an image. This is a major difference to single-source MDCT systems, which can provide similar temporal resolution by combining data from several heart cycles to an image in a multi-segment reconstruction. Then, however, temporal resolution strongly depends on the relation of heart rate and gantry rotation time. Meanwhile, several clinical studies have demonstrated the potential of DSCT to reliably perform coronary CT angiographic studies in patients with high and even irregular heart rates (e.g., Sun et al. 2011; Lee et al. 2012; Paul et al. 2013). DSCT is sufficiently accurate to diagnose clinically significant coronary artery disease in some or all difficult to image patients (Westwood et al. 2013). The good temporal resolution is also beneficial to reduce motion artifacts in cardiothoracic studies (e.g., Hutt et al. 2016).

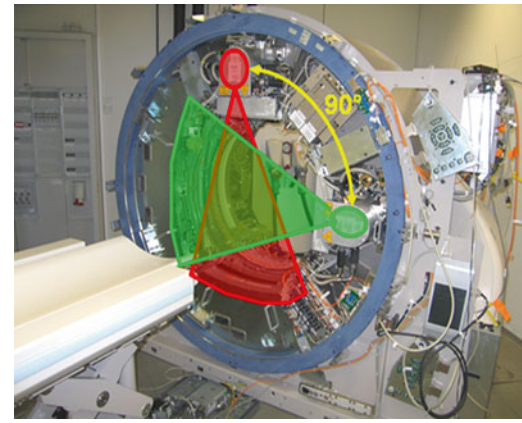

Fig. 9 DSCT with two independent measurement systems. The image shows the first-generation DSCT with an angle of 90° between both measurement systems. To increase the SFOV of detector B, a larger system angle of 95° was chosen for the second and third generations